HHS Public Access

Author manuscript

*Oncogene*. Author manuscript; available in PMC 2013 October 18.

Published in final edited form as:

*Oncogene*. 2013 April 18; 32(16): 2016–2026. doi:10.1038/onc.2012.218.

# Adhesion-mediated cytoskeletal remodeling is controlled by the direct scaffolding of Src from FAK complexes to lipid rafts by SSeCKS/AKAP12

**Bing Su**[1], **Lingqiu Gao**, **Fanjie Meng**[‡], **Li-wu Guo**[<], **Julian Rothschild**, and **Irwin H. Gelman**

Department of Cancer Genetics, Roswell Park Cancer Institute

## Abstract

Metastatic cell migration and invasion are regulated by altered adhesion-mediated signaling to the actin-based cytoskeleton via activated Src-FAK complexes. SSeCKS (the rodent orthologue of human Gravin/AKAP12), whose expression is downregulated by oncogenic Src and in many human cancers, antagonizes oncogenic Src pathways including those driving neovascularization at metastatic sites, metastatic cell motility and invasiveness. This is likely manifested through its function as a scaffolder of F-actin and signaling proteins such as cyclins, calmodulin, protein kinase (PK) C and PKA. Here, we show that in contrast to its ability to inhibit haptotaxis, SSeCKS increased prostate cancer cell adhesion to fibronectin (FN) and type I collagen in a FAK-dependent manner, correlating with a relative increase in $FAK^{poY397}$ levels. In contrast, SSeCKS suppressed adhesion-induced Src activation ($Src^{poY416}$) and phosphorylation of FAK at Y925, a known Src substrate site. SSeCKS also induced increased cell spreading, cell flattening, integrin β1 clustering and formation of mature focal adhesion plaques. An *in silico* analysis identified a Src-binding domain on SSeCKS (a.a.153–166) that is homologous to the Src binding domain of Caveolin-1, and this region is required for SSeCKS-Src interaction, for SSeCKS-enhanced Src activity and sequestration to lipid rafts, and for SSeCKS-enhanced adhesion of MAT-LyLu and CWR22Rv1 prostate cancer cells. Our data suggest a model in which SSeCKS suppresses oncogenic motility by sequestering Src to caveolin-rich lipid rafts, thereby disengaging Src from FAK-associated adhesion and signaling complexes.

### Keywords

Src; SSeCKS/Gravin/AKAP12; FAK; caveolin-1; adhesion; actin-based cytoskeleton



Address correspondence to: Irwin H Gelman, Roswell Park Cancer Institute, Elm and Carlton Streets, Buffalo, NY 14263. Tel.: 716-845-7681; Fax: 716-845-1698; irwin.gelman@roswellpark.org.

[1]current address: Shenzhen PKU-HKUST Medical Center, Shenzhen, Guangdong, China 518036

[‡]Department of Physiology and Biophysics, The State University of New York at Buffalo, Buffalo, NY 14214

[<]National Center for Toxicological Research, Jefferson, AR 72079

**Conflicts of Interest**

The authors declare that there are no competing conflicts of interest in relation to the current work.

## Introduction

Metastasis, recurrence and drug-resistance remain the major contributors to cancer-related mortality, spurring efforts to identify therapies that specifically target pathways that drive these parameters of malignancy (1). Members of the Src tyrosine kinase family (SFK) are known to be overexpressed and/or activated in many primary human cancers, typically through the activation of upstream growth factor receptor tyrosine kinases (2). However, the coincident activation of parallel oncogenic pathways suggests that SFK might be poor therapeutic targets in primary cancers (3,4). In contrast, there is a growing appreciation for the critical role played by SFK in controlling several parameters of cancer metastasis, such as tumor invasiveness and neovascularization at distal sites (5–8), and of drug-resistance (9–11).

The oncogenic potential of Src and Ras requires both potentiation of enzymatic activities (tyrosine kinase and GTPase functions, respectively) and specific localization to membrane sites (myristylation and palmitylation, respectively)(12–15). For example, mutation of Src's N-terminus to prevent myristylation ablates its oncogenic activity, even in the context of a constitutively-activated kinase domain (16). In contrast, splicing this myristylation signal onto AKT facilitates its membrane association and oncogenic activity (17). Indeed, Src requires N-terminal myristylation in order to enrich in specific lipid-raft membrane domains such as caveolae (18,19). The complex formed between Caveolin-1 (Cav-1), Src, second-messenger lipids and growth factor receptor tyrosine kinases is thought to mediate normal mitogenic downstream signals, endocytosis, cell-cell adhesion and interaction of the actin-based cytoskeleton with mechano-responsive structures on the plasma membrane (20,21). Although many cancers exhibit Cav-1 downregulation, the upregulation of Cav-1 in other cancers has been tied to increased oncogenic motility and invasiveness (21). A very recent model suggest that phosphorylation of Cav1 by Src on Y14 enables a dynamic, Rac1-dependent transient translocation of Cav1 from caveolae to focal adhesions, whereupon the dephosphorylation and subsequent degradation of Cav1 facilitates focal adhesion turnover and cell motility (22). Thus, Src-induced oncogenic motility may be facilitated by the increased rate of this pathway, correlating with a net downregulation of Cav1 levels.

SSeCKS (Src-suppressed C-kinase substrate), the rodent orthologue of human Gravin/AKAP12, seems to function as a metastasis suppressor via its ability to differentially scaffold signaling proteins such as protein kinase (PK) C, PKA, calmodulin and Src (23). SSeCKS also participates in the control of cytoskeletal reorganization associated with motility, most likely facilitated by domains that link it to both plasma membrane and cytoskeletal sites. Plasma membrane association is controlled by N-terminal myristylation and three N-terminal phosphoinositol-phosphate binding sites (24). SSeCKS/AKAP12 expression is often downregulated in human cancers, and it is especially downregulated due to promoter hypermethylation in metastatic lesions (23). The re-expression of SSeCKS in MAT-LyLu prostate cancer cells had little effect on the growth of primary-site tumors, but it suppressed the growth of spontaneous pulmonary metastases in part, by inhibiting tumor-encoded vascular endothelial growth factor (VEGF) secretion, thereby inhibiting neovascularization at metastatic sites (25). SSeCKS also inhibits oncogenic motility and invasiveness by disengaging growth factor-activated Src from activating PKC-Raf-MEK-

ERK pathways that control the formation of podosome/invadosome structures and that upregulate the expression/secretion of matrix metalloproteinases. Interestingly, Src autophosphorylation and substrate phosphorylation activity are not inhibited by SSeCKS, and taken together with the finding that SSeCKS alters actin-based cytoskeletal architecture, these data suggest that SSeCKS inhibits Src oncogenic signaling by physically scaffolding it away from downstream signal mediators.

Here we demonstrate the mechanism by which SSeCKS increases FAK-dependent cell adhesion to and spreading on Fibronectin (FN) and type I Collagen (Col I). SSeCKS-enhanced adhesion correlated with increased clustering of integrin β1 and formation of mature focal adhesion plaques. SSeCKS enhanced relative adhesion-induced FAKpoY397 levels, yet suppressed phosphorylation at FAK-Y925, a known Src substrate site (26), suggesting that Src is disengaged by SSeCKS from normal FAK/Src complexes. Consistent with this notion, we show that a direct binding between Src and SSeCKS via a domain (a.a. 153–166) homologous to the Src-binding site on Caveolin-1 (27) likely facilitates the enrichment of Src to caveolin-rich lipid rafts, concomitant with a relative increase in Cav-$1^{poY14}$ levels in these membrane domains. Our findings strongly suggest that SSeCKS attenuates Src's ability to induce metastatic progression by directly scaffolding Src pools from FAK complexes to lipid rafts, effectively suppressing formation of constitutive FAK/Src complexes that promote downstream signaling and cytoskeletal pathways.

## RESULTS

### SSeCKS-induced cell flattening and chemotaxis inhibition correlates with increased cell adhesion and spreading

Our previous data indicated that in addition to its ability to suppress metastasis *in vivo* by inhibiting tumor-derived expression of VEGF (25), SSeCKS also suppressed chemotaxis and oncogenic invasiveness (28). These functions and cell adhesion are governed by dynamic changes in actin cytoskeletal remodeling (29), and indeed, SSeCKS induces these changes in the context of cell flattening (23). Thus, we addressed whether SSeCKS could also alter adhesion and spreading when reexpressed in MAT-LyLu (MLL) prostate cancer cells. We confirmed the coincident effects of cell flattening and chemotaxis inhibition using MLL cells engineered for tetracycline-regulated ($tet_{OFF}$) SSeCKS reexpression (MLL/tet-SSeCKS (30), demonstrating a dose-dependent decrease in chemotaxis concomitant with cell flattening (supplemental fig. S1A and B) and the production of exaggerated pseudofilopodia projections (Fig. 1A). These data are consistent with our previous demonstrations that SSeCKS can normalize cytoskeletal structures such as actin stress fibers and mature focal adhesion plaques, and inhibit oncogenic motility parameters when reexpressed in Src- or Ras-transformed cancer cells (31,32).

We then addressed whether SSeCKS might also affect cell adhesion. Therefore, MLL/tet-SSeCKS cells grown in the presence or absence of tet (− or + SSeCKS, respectively) were adhered to ECM-coated plates, and both spreading and short-term adherence were assessed. SSeCKS induced 3.6- or 10-fold greater spreading activity on FN or Col I, respectively (Fig. 1B). In contrast, SSeCKS had no effect on cell spreading on vitronectin (VN) or laminin (LN) coated plates. Similar results were produced using long-term adhesion assays onto

ECM-coated plates (Fig. 1C), namely a dose-dependent increase in SSeCKS-induced adhesion to FN or Col I, but not to VN or LN. The SSeCKS-enhanced adhesion to FN was accompanied by increased cell flattening (Fig. 1D). Consistent with the notion that tumor cells have increased integrin-mediated cell migration (haptotaxis) to facilitate transverse migration through basement membranes (33), SSeCKS suppressed haptotactic motility towards FN- and Col I-, but not to VN- or LN-coated membranes (Fig. 1E).

## SSeCKS induces integrin β1 clustering

The ability of integrins to participate in cell-cell and cell-ECM interactions facilitates the altered adhesion and motility parameters that characterize cancer and metastatic cells, especially as this relates to the metastasis-related differential expression of specific integrins (34) and epithelial-to-mesenchymal transition (35). Moreover, integrins transduce adhesion-mediated signals to the actin-cytoskeleton via Src-FAK complexes in focal adhesions (36). Based on SSeCKS' ability to induce adhesion on FN (Fig. 1C), which involves β1 integrin (37), and based on previously data demonstrating activated β1 integrin in MLL prostate cancer cells (38), we addressed whether SSeCKS reexpression alters β1 levels. The relative levels of mature β1 were unaffected by SSeCKS reexpression in MLL/tet-SSeCKS cells, although SSeCKS slightly decreased the relative levels of uncleaved ("pre") β1 (Fig. 2A). Thus, the ability of SSeCKS to increase adhesion to FN is not due to overall changes in β1 expression. However, SSeCKS reexpression facilitated FN-induced β1 integrin clustering (as evidenced by punctate vs. homogeneous cytoplasmic β1 staining) as well as the formation of FAK- and vinculin-containing focal adhesion plaques and F-actin stress fibers (Fig. 2B). These effects were concomitant with significant SSeCKS-induced cell flattening. Attempts to demonstrate SSeCKS association with FAK or β1 using co-immunoprecipitation (IP) experiments were unsuccessful (data not shown). Taken together, these data suggest that SSeCKS facilitates adhesion on FN by remodeling β1 integrin/FAK complexes as well as their interaction with the actin-based cytoskeleton.

## SSeCKS-enhanced adhesion on FN is FAK-dependent

Integrin-mediated adhesion and motility signaling is regulated through the transient recruitment and activation of FAK-Src signaling complexes (39–41). To address whether FAK activity is critical to the SSeCKS-induced enhancement of FN-based adhesion, FAK +/+ and FAK−/− mouse embryo fibroblasts (MEF) were co-transfected with pEGFP plus either an SSeCKS expression plasmid or empty vector, and 40h later, GFP-positive cells were scored for their ability to adhere to FN-coated plates. The expression level of endogenous SSeCKS was roughly 5-fold higher in FAK−/− vs. FAK+/+ cells (Fig. 3A), and this correlated with >3-fold higher adhesion of FAK−/−(vector) cells than that of FAK+/+ (vector) cells on all concentrations of FN tested (Fig. 3B). The higher levels of ectopic SSeCKS expression in FAK−/− cells did not increase adhesion (Fig. 3B), suggesting that the higher basal SSeCKS levels in these cells may already be functionally saturated. In contrast, the ectopic expression of SSeCKS in FAK+/+ cells increased adhesion 2- to 3-fold over varying FN concentrations (Fig. 3B), paralleling the effect of either stable or transient SSeCKS expression in MLL cells (Figs. 1C and 3C, respectively). The co-expression of MLL cells with SSeCKS and FRNK, a natural FAK antagonist (42), suppressed the enhanced adhesion, whereas substitution of an inactive FRNK mutant, FRNK$^{S1034}$

("FRNKm"), negated FRNK's inhibitory effect (Fig. 3C). As a control, we showed that the relative expression levels of HA-tagged FRNK and FRNK$^{S1034}$ were similar in the transfected MLL cells (Fig. 3D).

FAK activity is thought to control adhesion turnover because FAK−/− MEF have increased numbers of vinculin-associated focal adhesions and display increased cell spreading (43). After adherence-induced integrin clustering, FAK autophosphorylates at Y397, forming an SH2 binding site for the recruitment of Src. The reciprocally activating FAK-Src complex induces the remodeling of the actin cytoskeleton that controls cell adhesion and motility (44). The dependence of this signaling on Src is evidenced by findings that motility induced by transgenic FAK expression in FAK-null fibroblasts is impaired by Src inhibition (45), and that activated Src rescues cell spreading in FAK−/− cells (46,47). We investigated whether the effects of SSeCKS on increased adhesion were mediated through FAK activation. Thus, serum-starved MLL/tet-SSeCKS grown overnight in the presence or absence of tet were either allowed to adhere to FN or kept in suspension ("sus"). SSeCKS induced an increase in the relative adhesion-induced level of FAK autophosphorylation (Fig. 4A). In contrast, SSeCKS decreased relative levels of adhesion-induced Src autophosphorylation (poY416) as well as phosphorylation on FAK at a major Src substrate site, Y925 (48) (Fig. 4A). The relative phosphorylation of FAK-Y861 (26) was unaffected by SSeCKS when normalized to total FAK protein levels. Adherence induced Mek activation, as demonstrated by relative phospho-Mek1/2 levels, was decreased by SSeCKS, paralleling the effect we showed previously by SSeCKS on serum-induced Mek activation (49). A failure to phosphorylate FAK$^{Y925}$ would prevent the formation of the SH2-mediated binding site for Grb2, and thus, prevent activation of Mek/Erk signaling associated with metastatic progression (50). Taken together with the data in Fig. 2B, these data suggest that SSeCKS interrupts adhesion-induced FAK-Src complex formation, disengaging it from both oncogenic actin cytoskeletal remodeling and activation of Mek/Erk signaling. This notion is backed up by the demonstration that SSeCKS re-expression decreases the amount of Src associating with FAK in co-IPs following adhesion to FN (Fig. 4B).

## SSeCKS may alter Src-FAK complex formation by directly scaffolding Src

Trevino et al. (51) recently reported that the siRNA-mediated knockdown of Src had little effect on primary tumor growth but greatly suppressed the formation of metastases, consistent with the known roles for Src in regulating oncogenic cell migration and invasiveness (52,53). SSeCKS, which is known to function as an antagonist of Src-induced oncogenic growth (31), did not alter the proliferation of MLL cells, he overall level of Src-induced substrate phosphorylation, or phosphorylation of specific Src substrates such as p130Cas (supplemental fig. S2) or Shc (49). This agrees with our previous results showing that SSeCKS reexpression could inhibit Src-induced anchorage- and growth factor-independence and Matrigel invasiveness without affecting Src tyrosine kinase activity (54,55).

The decreased level of adhesion-induced FAK$^{poY925}$ and the relative decrease in Src-FAK complex formation (Fig. 4C) after SSeCKS reexpression suggests that SSeCKS physically alters FAK-Src interaction. Multiple attempts at co-IP experiments between FAK and

SSeCKS showed no association (data not shown). However, Tao et al. (56) demonstrated that Src binds an N-terminal $^{12}$PxxP$^{15}$-containing domain on human SSeCKS, Gravin (Fig. 5A), which they posited was through Src's SH3 domain. This might suggest that SSeCKS prevents adhesion-induced FAK-Src complex formation by directly scaffolding Src. We confirmed that only an N-terminal SSeCKS domain encoding a.a. 2–274 could associate with Src in co-IP assays (Fig. 5B). To address whether this binding was Src-SH3 dependent, we produced full-length and P15A versions of His-tagged SSeCKS (supplemental fig. 3A), and showed that $Ni^{2+}$-beads charged with these proteins retained full binding activity to Src (Fig. 5C). This strongly suggests that the SSeCKS/Src interaction is not mediated through a classic SH3/ligand interaction, agreeing with the analysis that the SSeCKS$^{12}$PxxP$^{15}$ sequence does not conform to known SH3 ligand constraints (Kalle Saksela, personal communication).

*In silico* analysis identified an SSeCKS sequence, $^{154}$FKKVFKFVGFKTVK$^{165}$, that is homologous to the motif, ΦxxxΦxΦxxΦxx (Φ: hydrophobic residues), in Caveolin-1 (Cav1) (residues 82–101: DGIWKASFTTFTVTKYWFYR). This so-called Caveolin Scaffolding Domain (CSD) facilitates direct binding to H-Ras, Src family tyrosine kinases, PKC isoforms and the epidermal growth factor receptor (57), modulating at plasma membrane sites their roles in controlling oncogenic cell adhesion and migration (58). Deletion of a.a. 153–166 abrogated the ability of GST-SSeCKS[2–274] protein (supplemental fig. 3A) to pull down Src from cell lysates (Fig. 5D). Furthermore, the ability of purified His-Src and GST-SSeCKS[2–274] to efficiently bind each other in reciprocal co-IP assays required the putative Src-binding domain in a.a.153–166 (Fig. 5E). Importantly, whereas ectopic FL-SSeCKS could induce FN-mediated adhesion in MLL cells and in the human prostate cancer cell line, CWR22Rv1, SSeCKS deleted of the a.a. 153–166 domain (supplemental fig. 3B) failed to enhance attachment (Fig. 5F). These data indicate that SSeCKS likely binds Src via its N-terminal Cav-1-like motif and not via the putative PxxP ligand motif, and that an SSeCKS-Src interaction facilitates the enhanced attachment on FN by prostate cancer cells.

## SSeCKS sequesters Src from FAK-Src complexes

Beside the CSD, Src association with caveolae is facilitated by its N-terminal myristylation (15), and indeed, Cav1 was first identified as a v-Src substrate (59,60). SSeCKS is also myristylated at its N-terminus (61), and therefore, it is conceivable that SSeCKS may function in a similar fashion to scaffold Src to lipid raft sites (and away from sites of adhesion-mediated FAK activation such as focal adhesion plaques) via its CSD-like domain. This would be especially significant in that caveolae coordinate cell migration by enriching major signaling mediators in plasma membrane microdomains in a spatiotemporal fashion (62). To address this, we plated serum-starved MLL/tet-SSeCKS cells grown overnight in the presence or absence of tet onto FN for 60 min (vs. suspended cells), and then subjected TRITON-X100 lysates to sucrose density gradients. Lipid rafts, as marked by the enrichment of Cav1, are typically found in lighter membrane fractions 4–5 in adherent cells but in heavier fractions in suspended MLL cells (Fig. 6A). SSeCKS did not significantly alter the localization of Cav1 in adherent cells, but did shift Cav1 to lighter fractions 4 and 5 in suspended cells. This corresponded to a similar shift of the ectopic SSeCKS in both suspended and adherent cells to lighter fractions (fraction 5 for the suspended cells and

fractions 4–5 for the adherent cells). Although SSeCKS had no effect of FAK localization in either adherent or suspended cells (with FAK enriching in fractions 6–9), SSeCKS induced a shift in Src in both suspended and adherent cells to lighter fractions (5 in suspended cells and 4–5 in adherent cells). Thus, SSeCKS induced a movement of some Src from fractions containing FAK to those containing Cav1.

SSeCKS also induced increased relative Cav1$^{poY14}$ levels in adherent cells, specifically a two-fold increase in fractions 4 and 5, which are enriched with ectopic SSeCKS and Src (Fig. 6A). A similar increase in relative Cav1$^{poY14}$ levels was detected in total cell lysates of adherent MLL/tet-SSeCKS cells (supplemental fig. 4; compare lanes C and D). As a control, treatment with methyl-∃-cyclodextrin (MbCD), a cholesterol-binding compound that dissolves caveolae (63), induced movement of Cav1 and Cav1$^{poY14}$ into slightly heavier fractions (out of fraction 3 or 4, respectively, in adherent cells). MbCD induced a much greater egress of SSeCKS and Src from lighter fractions. These data suggest that SSeCKS scaffolds Src to caveolin-rich lipid rafts in adherent cells, resulting in increased Cav1 tyrosine phosphorylation. Consistent with this model, the ability of SSeCKS to induce Src activity in lipid rafts and at general membrane sites using fluorescence resonance energy transfer (FRET) sensors (64,65) required SSeCKS' Src-binding domain (Fig. 6B; fig. S6). In contrast, SSeCKS did not activate FAK in lipid rafts, consistent with the notion that FAK remains enriched in focal adhesions during adhesion and that SSeCKS does not directly regulate its activity.

## DISCUSSION

Although there are rare cases of breast and colon cancers expressing Src containing activating mutations akin to the so-called "viral Src signature" (66,67), Src likely drives oncogenic progression by virtue of being overexpressed or activated by upstream growth factor receptors (68,69). Many parameters of metastasis seem to be dependent on Src signaling, such as oncogenic motility, recruitment of mural cells to metastatic niches, and neovascularization at metastatic sites (6), leading to a renewed focus on Src as a therapeutic target in advanced cancer. Our data indicate that SSeCKS functions as an especially potent suppressor of Src's metastasis-promoting functions, even though SSeCKS does not inhibit Src's intrinsic tyrosine kinase activity (55,70). Here, we show that SSeCKS attenuates adhesion-induced activation of Src (based on poY416 levels), but more potently suppresses phosphorylation of FAK$^{Y925}$, a known Src substrate site, following FN-mediated adhesion. This would prevent the formation of a ligand site for Grb2-SH2, and the subsequent activation of downstream Mek-Erk pathways. These data are similar to those showing that SSeCKS suppresses growth factor-induced oncogenic invasiveness pathways through the disengagement of Src from Mek-Erk pathways (49).

Our data demonstrate concurrence between SSeCKS-induced cell flattening, previously shown as mediated through the remodeling of the actin-based cytoskeleton (71), increased cell adhesion to and spreading on FN, and increased relative FAK autophosphorylation levels. The ability of SSeCKS to decrease adhesion-induced Src activation and relative FAK$^{poY925}$ levels suggests that SSeCKS disengages Src from the FAK/Src complexes that drive oncogenic adhesion signals, concomitant with decreased focal turnover. In a previous

study (49), SSeCKS did not alter serum-induced FAK or Src activation levels, but it did suppress the relative levels of Mek activation, again, suggesting that SSeCKS disengages Src from downstream signaling, in this case, pathways driving oncogenic invasiveness and chemotaxis. In this model, the SSeCKS-induced disengagement of Src would increase the relative level of adhesion-activated FAK (reflected in relative $FAK^{poY397}$ levels). This agrees with previous data from Yeo et al. (72) showing that expression of a Src SH2 domain mutant, R175L, which is prevented from binding to autophosphorylated FAK, results in higher relative adhesion-induced $FAK^{poY397}$ levels.

Although SSeCKS might alter Src compartmentalization indirectly through its ability to remodel the cytoskeleton, we addressed whether there is a direct scaffolding function for Src, made likely by previous data that the proline 15/16 residues of Gravin are required for its association with Src in complex containing ($\exists_2$adrenergic receptor (56). Indeed, our data indicate that SSeCKS binds Src directly through an N-terminal fragment (a.a. 2–274). However, in our hands, both this fragment and a P15A mutant bound equally well to Src, suggesting that the this is not a classic SH3/PxxP interaction. A subsequent *in silico* analysis identified another motif within the SSeCKS N-terminus (a.a. 153–166) that is homologous to the caveolin binding domain for Src. Importantly, deletion of this domain abrogated SSeCKS-Src association and the ability of SSeCKS to enhance Src activity in lipid rafts as well as adhesion of prostate cancer cells.

There is growing evidence that the ability of Src to induce oncogenic signaling for proliferation, cell survival, and cell motility might relate to an imbalance in its shuttling between lipid rafts and cell-cell or focal adhesion complexes. For example, sequestration of Src by the Csk-binding protein, Cbp, to lipid rafts suppresses oncogenic transformation (73). A recent study by Nethe and Hordijk (74) suggests that during normal adhesion signaling, Src shuttling to lipid rafts induces Cav-1 Y14 phosphorylation followed by a secondary Rac1-dependent translocation of Src/$Cav\text{-}1^{poY14}$ to FAK-enriched focal adhesion plaques. A subsequent dephosphorylation and degradation of Cav-1 then triggers focal adhesion turnover associated with cell motility. Another layer of control is added by the findings of del Pozo et al. (75), who showed that cell detachment induces translocation of $Cav\text{-}1^{poY14}$ to caveolae followed by caveolar endocytosis.

Our compatible model (Fig. 7) suggests that SSeCKS facilitates the initial Src translocation to caveolin-rich lipid rafts, likely mediated by SSeCKS' N-terminal myristyl group, and possibly acts as a licensing factor for the amount of Src/Cav-1 that might be able to move to focal adhesions. Conditions of SSeCKS deficiency, such as in cancer, would shift more association of Src/Cav-1 to the focal adhesions, resulting in both increased focal adhesion plaque turnover and Cav-1 degradation. Indeed, our data show that MLL cells lacking SSeCKS express roughly twofold lower total Cav-1 protein levels which are increased after SSeCKS re-expression (Fig. 6A, supplemental fig. S4), and that SSeCKS re-expression rescues the formation of mature, stable focal adhesion plaques (Fig. 2). Consistent with this model, the re-expression of SSeCKS in adherent MLL induced the translocation of Src to lighter sucrose gradient fractions containing Cav-1 but no $FAK^{poY397}$. This enrichment of SSeCKS/Src in lipid rafts resulted in increased relative $Cav\text{-}1^{poY14}$ levels. In contrast, in the absence of SSeCKS, significant pools of Src and $Cav\text{-}1^{poY14}$ co-fractionated with

FAK$^{poY397}$, yet almost none was found in the typical lipid raft fractions. Interestingly, whereas saturated binding of Cav-1 to Src inhibits its intrinsic kinase activity (27), binding by SSeCKS does not, and indeed, SSeCKS seems to enhance Src's ability to phosphorylate Cav-1 in lipid raft fractions. This implies that the function of Src in lipid rafts is dynamic, depending on subtle interactions with either SSeCKS or Cav-1. Taken together, these data are consistent with a model in which the scaffolding of Src by SSeCKS to caveolin-rich lipid rafts modulates the amount of Src/Cav-1$^{poY14}$ that can translocate to FAK-containing focal adhesion complexes, thereby attenuating downstream oncogenic signaling.

## Experimental Procedures

### Antibodies and reagents

The following primary antibodies (Ab) were used: rabbit polyclonals specific for integrin β1, FAK$^{poY861}$, FAK$^{poY925}$, MEK1, His-Tag, GAPDH (Santa Cruz Biotechnology, Santa Cruz, CA) or CAS (BD Transduction Laboratories); mouse MAb specific for HA-epitope tag (Applied Biological Materials), Src, Src$^{poY416}$, MEK1/2$^{poS217/221}$, CAS$^{poY165}$, Cav-1$^{poY14}$ (Cell Signaling Technology, Beverly, MA) or vinculin (Sigma). F-actin was stained with rhodamine-phalloidin (Sigma). Caveolae/Rafts isolation kit and methyl-β-cyclodextrin (MbCD) were purchased from Sigma (St. Louis, MO).

### Cell culture

MLL cell lines expressing tetracycline-regulated (tet$_{OFF}$) SSeCKS (MLL/tet-SSeCKS) were described previously (30). The cells were maintained in Dulbecco's modified Eagle's media (DMEM) supplemented with 10% bovine serum (BS) and 0.7μg/ml tetracycline. CWR22rv1 cells were maintained in RPMI1640 media supplemented with 10% fetal bovine serum (fBS).

### Adhesion assay

Cell adhesion experiments were performed as described in (76). In brief, 96-well microtiter plates were coated with 0.1 ml of extracellular matrix protein (ECM: FN, vitronectin, laminin or Col-I), incubated at room temperature (RT) for 1 h, and blocked by 10mg/ml BSA at RT for 0.5 h after washing. Cells ($1.5 \times 10^4$) were added to each coated well and incubated at 37 °C followed by fixing with 5% glutaraldehyde and staining with crystal violet after two washes. The absorbance of each well was measured at 570 nm. The data were expressed as the mean of triplicate wells. For assessment of cell spreading on ECM, images from adherent cells were taken at 30, 60, 90, and 120 min after seeding. Image J (http://rsbweb.nih.gov/ij/) was used to quantify cell spreading as described by Ross et al. (77). In brief, measurements were taken from at least three different fields of view with a minimum of ten cells per field. Areas were measured in pixels and the spreading index was determined by standardizing the spreading of cells to the mean size of cells under control conditions.

### Haptotaxis assays

Modified Boyden chamber assays were performed to assess haptotaxis by using a polyethylene terephthalate tissue culture insert with 8-μm pores (Becton Dickinson, Franklin

Lakes, NJ). $3 \times 10^4$ cells in 100 μl of serum-free DMEM were seeded atop membranes coated on their bottoms with serum-free ECM protein as an attractant. The cells were allowed to migrate overnight, and cells that had not penetrated the filters were removed by scrubbing with cotton swabs. The chambers were fixed and stained using Diff-Quik Stain Set (Dade Behring Inc., Newark, DE), and examined under a bright-field microscope. Values for migration were obtained by counting 6 fields of at least 80 cells/field per membrane and represent the average of three independent experiments.

### Western blotting (IB)

MLL/tet-SSeCKS cells grown in the presence or absence of tet (0.7 μg/ml) were plated in 10 cm dishes, serum-starved overnight, trypsinized, resuspended in DMEM containing soybean anti-trypsin inhibitor (Sigma), and either kept in suspension or re-plated onto FN-coated dishes (10 μg/ml) for various durations. Cells were lysed in RIPA buffer (61) supplemented with 10 mM $Na_3VO_4$, 1 mM NaF, and Complete Protease Inhibitor Cocktail (Roche Diagnostics, Mannheim, Germany). 40 μg of total protein per sample was subjected to SDS-PAGE, blotted onto PVDF membranes which were blocked for 30 min with 5% bovine serum albumin (Sigma) in 1×TBS/T (0.1% Tween-20 in Tris-buffered saline) and then probed and washed as described previously (61). Digital imaging and signal quantification were performed on a Chemi-Genius$^2$ Bio-Imager using GeneTools software (Syngene, Frederick, MD).

### Immunofluorescence Analysis

MLL/tet-SSeCKS cells plated on glass coverslips (22 $mm^2$) coated with FN for 90 min in the presence or absence of tet were fixed at −20°C for 20 min with 60% acetone/3.7% paraformaldehyde in PBS, and blocked with 3% non-fat dry milk in PBS for 30 min at RT. Cells were incubated with primary Rb-PAbs against integrin β1 (1:100) or FAK (1:150), washed and then incubated with DAPI (Invitrogen; 1:500) and FITC-conjugated goat anti-rabbit IgG (1:250; Chemicon, Temecula, CA). Fluorescent images were captured using Nikon TE2000-E inverted microscope equipped with a Roper CoolSnap HQ CCD camera.

### Cell lines

FAK+/+[SSeCKS] or FAK−/−[SSeCKS] expresser cell lines were produced by infecting with pBABE-SSeCKS (25) retrovirus packaged in 293GPG cells (78) and then selecting in 2 μg/mL puromycin. MLL/tet-SSeCKS[FRNK] or FRNKm expressor cell lines were produced by transfecting with 2 μg of DNA (pcDNA3.1-FRNK-HA or pcDNA3.1-FRNK-(Ser1038)-HA in Lipofectamine 2000 (Invitrogen) and selecting in 200 μg/ml hygromycin.

### Cell viability

Cell proliferation was evaluated using colorimetric MTS assay (Promega) that measures restoration of 3-(4,5-dimethylthiazol-2-yl)-5-(3-carboxymethoxyphenyl)-2-(4-sulfophenyl)-2H-tetrazolium (MTS) to formazan by metabolically active cells. The absorbance of the formazan at 490 nm was determined using a microplate reader in tissue culture medium following 24h, 48h, 72h incubation with or without tet. The results are expressed as mean values ± standard deviation for two independent experiments.

### Plasmid constructs

SSeCKS constructs containing the Δ153–166 deletion in either GST-SSeCKS[a.a.2–274] or pcDNA3.1/αSSeCKS-GFP were produced by a long range inverse PCR technique we described previously (79) using “153" and “166" primers containing an SpeI site (underlined): “153" primer 5’-ATGCACTAGTGCCAACATCATTAGCCTGGGA-3'; “166" primer- 5’-GCGCACTAGTACGGTGAAGAAGGATAAAAATGAA -3'. SSeCKS constructs containing Pro15Ala mutation in either pBABE-SSeCKS or pHis-TAT-SSeCKS (80) were produced by a PCR-mediated mutagenesis (QuikChange Site-Directed Mutagenesis Kit, Stratagene) using primers: SSeCKS-Pro15AlaF: 5’-AGCCCCGAGCAGGCGGCGGGGAGCGAC -3’ and SSeCKS-Pro15AlaR: 5’-GTCGCTCCCCGCCGCCTGCTCGGGGCT – 3’.

### Pulldown assay

Lysates containing 500 μg of protein from NIH3T3/c-Src cells were incubated with glutathione Sepharose 4B beads bound to GST or various GST-SSeCKS fusion proteins described previously (70). After washing twice in RIPA buffer, the beads were subjected to IB analysis and probed with anti-Src rabbit Ab. Lysates of NIH3T3/c-Src cells were incubated with $Ni^{2+}$-beads bound to His-SSeCKS (full length or P15A) proteins or glutathione Sepharose 4B beads bound to GST, GST-SSeCKS[a.a.2–274] or GST-SSeCKS[a.a.2–274Δ153–166] proteins. After washing twice in RIPA lysis buffer, the beads were subjected to IB analysis and probed with anti-Src rabbit Ab.

### Isolation of Caveolin-rich membrane fractions

The experiments were performed using a Sigma kit (CS0750) following cmanufacturer protocols. Briefly, MLL/tet-SSeCKS cells incubated overnight with or without tet were kept in suspension or adhered to FN-coated wells (10 μg/ml) for 1h, washed twice with ice-cold PBS and lysed with Sigma lysis buffer (L7667) containing 1% TRITON X-100. The lysates were transferred to a pre-cooled microcentrifuge tube, incubated on ice for 30 min, adjusted to 40% sucrose in lysis buffer, and placed on the bottom of an ultracentrifuge tube. A 5–30% linear sucrose gradient was formed above the samples and then centrifuged in an SW41 rotor (Beckman) at 46,000 rpm for 4 h at 4 °C. One ml fractions were collected across the entire gradient, and equal amounts of total protein (40 μg/lane) were analyzed by IB. Caveolae were interrupted by treatment with the cholesterol-binding agent MbCD (10 mM) for 1 h during FN stimulation.

### Fluorescence resonance emission transfer (FRET) analysis

Images were obtained using an inverted Zeiss Axio Observer A1 equipped with an Andor iXon DV897 back-illuminated cooled CCD camera (Andor, CT, USA). The images at the donor emission and acceptor emission were recorded through a Dual View (Photometrics) splitter with double band excitation filters. An LED light engine from Lumencor (Lumencor, San Francisco, CA) was used for excitation at wavelengths of 433 nm for the donor and 515 nm for acceptor. FRET ratios were calculated as the energy transfer index: FRET Ratio = $(I_A - I_{Dbt})/I_D$, where $I_A$ is the peak acceptor emission signal of FRET, $I_D$ is the peak donor

emission signal and $I_{Dbt}$ is the signal in the acceptor channel due to donor signal bleed-through as described previously (81)

## Supplementary Material

Refer to Web version on PubMed Central for supplementary material.

## ACKNOWLEDGEMENTS

We thank Toru Ouchi and Eugene Kandel for critical review of the manuscript, Kalle Saksela and Bruce Mayer for discussions on SH3 interactions and Bruce Mayer, Y. Peter Wang and Tom Parsons for reagents. This work is supported by grants (I.H.G.) CA94108, CA116430 (NIH/NCI), PC074228, PC101210 (DoD), and in part, through NCI Comprehensive Cancer funds (P30-CA016056).

## REFERENCES

1. Iiizumi M, Liu W, Pai SK, Furuta E, Watabe K. Drug development against metastasis-related genes and their pathways: A rationale for cancer therapy. Biochim Biophys Acta. 2008; 1786:87–104. [PubMed: 18692117]
2. Frame MC. Newest findings on the oldest oncogene; how activated src does it. J Cell Sci. 2004; 117:989–998. [PubMed: 14996930]
3. Bild AH, Parker JS, Gustafson AM, Acharya CR, Hoadley KA, Anders C, et al. An integration of complementary strategies for gene-expression analysis to reveal novel therapeutic opportunities for breast cancer. Breast Cancer Res. 2009; 11:R55. [PubMed: 19638211]
4. Kumar A, White TA, Mackenzie AP, Clegg N, Lee C, Dumpit RF, et al. Exome sequencing identifies a spectrum of mutation frequencies in advanced and lethal prostate cancers. Proc Natl Acad Sci U S A. 2011; 108:17087–17092. [PubMed: 21949389]
5. Sturge J, Caley MP, Waxman J. Bone metastasis in prostate cancer: emerging therapeutic strategies. Nat Rev Clin Oncol. 2011; 8:357–368. [PubMed: 21556025]
6. Gelman IH. Src-family tyrosine kinases as therapeutic targets in advanced cancer. Front Biosci. 2011; E3:801–807.
7. Trevino JG, Summy JM, Lesslie DP, Parikh NU, Hong DS, Lee FY, et al. Inhibition of SRC expression and activity inhibits tumor progression and metastasis of human pancreatic adenocarcinoma cells in an orthotopic nude mouse model. Am J Pathol. 2006; 168:962–972. [PubMed: 16507911]
8. Eliceiri BP, Paul R, Schwartzberg PL, Hood JD, Leng J, Cheresh DA. Selective requirement for Src kinases during VEGF-induced angiogenesis and vascular permeability. Molecular Cell. 1999; 4:915–924. [PubMed: 10635317]
9. Hiscox S, Morgan L, Green T, Nicholson RI. Src as a therapeutic target in anti-hormone/anti-growth factor-resistant breast cancer. Endocr Relat Cancer. 2006; 13(Suppl 1):S53–S59. S53–S59. [PubMed: 17259559]
10. Ischenko I, Camaj P, Seeliger H, Kleespies A, Guba M, De Toni EN, et al. Inhibition of Src tyrosine kinase reverts chemoresistance toward 5-fluorouracil in human pancreatic carcinoma cells: an involvement of epidermal growth factor receptor signaling. Oncogene. 2008; 27:7212–7222. [PubMed: 18794807]
11. Yoshida T, Okamoto I, Okamoto W, Hatashita E, Yamada Y, Kuwata K, et al. Effects of Src inhibitors on cell growth and epidermal growth factor receptor and MET signaling in gefitinib-resistant non-small cell lung cancer cells with acquired MET amplification. Cancer Sci. 2010; 101:167–172. [PubMed: 19804422]
12. Martin GS. The hunting of the Src. Nature Reviews Molecular Cell Biology. 2001; 2:467–475. [PubMed: 11389470]
13. Bos JL. ras oncogenes in human cancer: a review. Cancer Res. 1989; 49:4682–4689. [PubMed: 2547513]

14. Milligan G, Parenti M, Magee AI. The dynamic role of palmitoylation in signal transduction. TIBS. 1995; 20:181–186. [PubMed: 7610481]
15. Resh MD. Myristylation and Palmitylation of src family members: The fats of the matter. Cell. 1994; 76:411–414. [PubMed: 8313462]
16. Cross FR, Garber EA, Pellman D, Hanafusa H. A short sequence in the p60src N terminus is required for p60src myristylation and membrane association and for cell transformation. Mol Cell Biol. 1984; 4:1834–1842. [PubMed: 6092942]
17. Aoki M, Batista O, Bellacosa A, Tsichlis P, Vogt PK. The akt kinase: molecular determinants of oncogenicity. Proc Natl Acad Sci U S A. 1998; 95:14950–14955. [PubMed: 9843996]
18. Song KS, Sargiacomo M, Galbiati F, Parenti M, Lisanti MP. Targeting of a $G_{\alpha}$ subunit ($G_{i1\alpha}$) and c-Src tyrosine kinase to caveolae membranes: Clarifying the role of N- myristoylation. Cell Mol Biol. 1997; 43:293–303. [PubMed: 9193783]
19. Wanaski SP, Ng BK, Glaser M. Caveolin scaffolding region and the membrane binding region of src form lateral membrane domains. Biochemistry. 2003; 42:42–56. [PubMed: 12515538]
20. Sverdlov M, Shajahan AN, Minshall RD. Tyrosine phosphorylation-dependence of caveolae-mediated endocytosis. J Cell Mol Med. 2007; 11:1239–1250. [PubMed: 18205698]
21. Patra SK. Dissecting lipid raft facilitated cell signaling pathways in cancer. Biochim Biophys Acta. 2008; 1785:182–206. [PubMed: 18166162]
22. Nethe M, Hordijk PL. A model for phospho-caveolin-1-driven turnover of focal adhesions. Cell Adh Migr. 2011; 5:59–64. [PubMed: 20948305]
23. Gelman IH. Emerging Roles for SSeCKS/Gravin/AKAP12 in the Control of Cell Proliferation, Cancer Malignancy, and Barriergenesis. Genes & Cancer. 2010; 1:1147–1156. [PubMed: 21779438]
24. Yan X, Walkiewicz M, Carlson J, Leiphon L, Grove B. Gravin dynamics regulates the subcellular distribution of PKA. Exp Cell Res. 2009; 315:1247–1259. [PubMed: 19210988]
25. Su B, Zheng Q, Vaughan MM, Bu Y, Gelman IH. SSeCKS metastasis-suppressing activity in MatLyLu prostate cancer cells correlates with VEGF inhibition. Cancer Res. 2006; 66:5599–5607. [PubMed: 16740695]
26. Brunton VG, Avizienyte E, Fincham VJ, Serrels B, Metcalf CA III, Sawyer TK, et al. Identification of Src-specific phosphorylation site on focal adhesion kinase: dissection of the role of Src SH2 and catalytic functions and their consequences for tumor cell behavior. Cancer Res. 2005; 65:1335–1342. [PubMed: 15735019]
27. Li SW, Couet J, Lisanti MP. Src tyrosine kinases, $G_{\alpha}$ subunits, and H-Ras share a common membrane-anchored scaffolding protein, caveolin - Caveolin binding negatively regulates the auto-activation of Src tyrosine kinases. J Biol Chem. 1996; 271:29182–29190. [PubMed: 8910575]
28. Su B, Bu Y, Engelberg D, Gelman IH. SSeCKS/Gravin/AKAP12 inhibits cancer cell invasiveness and chemotaxis by suppressing a protein kinase C- Raf/MEK/ERK pathway. J Biol Chem. 2010; 285:4578–4586. [PubMed: 20018890]
29. Pollard TD, Borisy GG. Cellular motility driven by assembly and disassembly of actin filaments. Cell. 2003; 112:453–465. [PubMed: 12600310]
30. Xia W, Unger P, Miller L, Nelson J, Gelman IH. The *Src*-suppressed C kinase substrate, SSeCKS, is a potential metastasis inhibitor in prostate cancer. Cancer Rese. 2001; 61:5644–5651.
31. Lin X, Gelman IH. Re-expression of the major protein kinase C substrate, SSeCKS, suppresses v-*src*-induced morphological transformation and tumorigenesis. Cancer Res. 1997; 57:2304–2312. [PubMed: 9187136]
32. Xia W, Gelman IH. Mitogen- and FAK-regulated tyrosine phosphorylation of the SSeCKS scaffolding protein modulates its actin-binding properties. Exp Cell Res. 2002; 277:139–151. [PubMed: 12083796]
33. Damsky CH, Werb Z. Signal transduction by integrin receptors for extracellular matrix: cooperative processing of extracellular information. Curr Opin Cell Biol. 1992; 4:772–781. [PubMed: 1329869]
34. Mizejewski GJ. Role of integrins in cancer: survey of expression patterns. Proc Soc Exp Biol Med. 1999; 222:124–138. [PubMed: 10564536]

35. Yilmaz M, Christofori G. EMT, the cytoskeleton, and cancer cell invasion. Cancer Metastasis Rev. 2009; 28:15–33. [PubMed: 19169796]
36. Playford MP, Schaller MD. The interplay between Src and integrins in normal and tumor biology. Oncogene. 2004; 23:7928–7946. [PubMed: 15489911]
37. Kumar CC. Signaling by integrin receptors. Oncogene. 1998; 17:1365–1373. [PubMed: 9779984]
38. MacCalman CD, Brodt P, Doublet JD, Jednak R, Elhilali MM, Bazinet M, et al. The loss of E-cadherin mRNA transcripts in rat prostatic tumors is accompanied by increased expression of mRNA transcripts encoding fibronectin and its receptor. Clin Exp Metastasis. 1994; 12:101–107. [PubMed: 8306523]
39. Mitra SK, Schlaepfer DD. Integrin-regulated FAK-Src signaling in normal and cancer cells. Curr Opin Cell Biol. 2006; 18:516–523. [PubMed: 16919435]
40. Brunton VG, Frame MC. Src and focal adhesion kinase as therapeutic targets in cancer. Curr Opin Pharmacol. 2008; 8:427–432. [PubMed: 18625340]
41. Zhao J, Guan JL. Signal transduction by focal adhesion kinase in cancer. Cancer Metastasis Rev. 2009; 28:35–49. [PubMed: 19169797]
42. Schaller MD, Borgman CA, Parsons JT. Autonomous expression of a noncatalytic domain of the focal adhesion-associated protein tyrosine kinase pp125FAK. Mol Cell Biol. 1993; 13:785–791. [PubMed: 8423801]
43. Ilic D, Furuta Y, Kanazawa S, Takeda N, Sobue K, Nakatsuji N, et al. Reduced cell motility and enhanced focal adhesion contact formation in cells from FAK-deficient mice. Nature. 1995; 377:539–544. [PubMed: 7566154]
44. Schlaepfer DD, Hauck CR, Sieg DJ. Signaling through focal adhesion kinase. Prog Biophys Mol Biol. 1999; 71:435–478. [PubMed: 10354709]
45. Sieg DJ, Hauck CR, Schlaepfer DD. Required role of focal adhesion kinase (FAK) for integrin-stimulated cell migration. J Cell Sci. 1999; 112(Pt 16):2677–2691. [PubMed: 10413676]
46. Richardson A, Malik RK, Hildebrand JD, Parsons JT. Inhibition of cell spreading by expression of the C-terminal domain of focal adhesion kinase (FAK) is rescued by coexpression of Src or catalytically inactive FAK: a role for paxillin tyrosine phosphorylation. Mol Cell Biol. 1997; 17:6906–6914. [PubMed: 9372922]
47. Moissoglu K, Gelman IH. v-Src Rescues Actin-Based Cytoskeletal Architecture and Cell Motility, and Induces Enhanced Anchorage-Independence During Oncogenic Transformation of FAK-Null Fibroblasts. J Biol Chem. 2003; 278:47946–47959. [PubMed: 14500722]
48. Schlaepfer DD, Hunter T. Evidence for in vivo phosphorylation of the Grb2 SH2-domain binding site on focal adhesion kinase by Src-family protein-tyrosine kinases. Mol Cell Biol. 1996; 16:5623–5633. [PubMed: 8816475]
49. Su B, Bu Y, Engelberg D, Gelman IH. SSeCKS/Gravin/AKAP12 inhibits cancer cell invasiveness and chemotaxis by suppressing a PKC-RAF/MEK/ERK pathway. J Biol Chem. 2010; 285:4578–4586. [PubMed: 20018890]
50. Mitra SK, Mikolon D, Molina JE, Hsia DA, Hanson DA, Chi A, et al. Intrinsic FAK activity and Y925 phosphorylation facilitate an angiogenic switch in tumors. Oncogene. 2006; 25:5969–5984. [PubMed: 16682956]
51. Trevino JG, Summy JM, Lesslie DP, Parikh NU, Hong DS, Lee FY, et al. Inhibition of SRC expression and activity inhibits tumor progression and metastasis of human pancreatic adenocarcinoma cells in an orthotopic nude mouse model. Am J Pathol. 2006; 168:962–972. [PubMed: 16507911]
52. Frame MC. Newest findings on the oldest oncogene; how activated src does it. J Cell Sci. 2004; 117:989–998. [PubMed: 14996930]
53. Martin GS. The hunting of the Src. Nat Rev Mol Cell Biol. 2001; 2:467–475. [PubMed: 11389470]
54. Lin X, Gelman IH. Reexpression of the major protein kinase C substrate, SSeCKS, suppresses v-src-induced morphological transformation and tumorigenesis. Cancer Res. 1997; 57:2304–2312. [PubMed: 9187136]
55. Gelman IH, Gao L. SSeCKS/Gravin/AKAP12 metastasis suppressor inhibits podosome formation via RhoA- and Cdc42-dependent pathways. Mol Cancer Res. 2006; 4:151–158. [PubMed: 16547152]

56. Tao J, Wang HY, Malbon CC. Src docks to A-kinase anchoring protein gravin, regulating beta2-adrenergic receptor resensitization and recycling. J Biol Chem. 2007; 282:6597–6608. [PubMed: 17200117]
57. Razani B, Woodman SE, Lisanti MP. Caveolae: from cell biology to animal physiology. Pharmacol Rev. 2002; 54:431–467. [PubMed: 12223531]
58. Navarro A, Anand-Apte B, Parat MO. A role for caveolae in cell migration. FASEB J. 2004; 18:1801–1811. [PubMed: 15576483]
59. Glenney JR Jr. Tyrosine phosphorylation of a 22-kDa protein is correlated with transformation by Rous sarcoma virus. J Biol Chem. 1989; 264:20163–20166. [PubMed: 2479645]
60. Rothberg KG, Heuser JE, Donzell WC, Ying YS, Glenney JR, Anderson RG. Caveolin, a protein component of caveolae membrane coats. Cell. 1992; 68:673–682. [PubMed: 1739974]
61. Lin X, Tombler E, Nelson PJ, Ross M, Gelman IH. A novel *src*- and *ras*-suppressed protein kinase C substrate associated with cytoskeletal architecture. J Biol Chem. 1996; 271:28430–28438. [PubMed: 8910468]
62. Shaul PW, Anderson RG. Role of plasmalemmal caveolae in signal transduction. Am J Physiol. 1998; 275:L843–L851. [PubMed: 9815100]
63. Williams TM, Lisanti MP. Caveolin-1 in oncogenic transformation, cancer, and metastasis. Am J Physiol Cell Physiol. 2005; 288:C494–C506. [PubMed: 15692148]
64. Seong J, Ouyang M, Kim T, Sun J, Wen PC, Lu S, et al. Detection of focal adhesion kinase activation at membrane microdomains by fluorescence resonance energy transfer. Nat Commun. 2011; 2:406. [PubMed: 21792185]
65. Seong J, Lu S, Ouyang M, Huang H, Zhang J, Frame MC, et al. Visualization of Src activity at different compartments of the plasma membrane by FRET imaging. Chem Biol. 2009; 16:48–57. [PubMed: 19171305]
66. Malek RL, Irby RB, Guo QBM, Lee K, Wong S, He M, et al. Identification of Src transformation fingerprint in human colon cancer. Oncogene. 2002; 21:7256–7265. [PubMed: 12370817]
67. Irby RB, Mao WG, Coppola D, Kang J, Loubeau JM, Trudeau W, et al. Activating SRC mutation in a subset of advanced human colon cancers. Nature Genet. 1999; 21:187–190. [PubMed: 9988270]
68. Mao WG, Irby R, Coppola D, Fu L, Wloch M, Turner J, et al. Activation of c-Src by receptor tyrosine kinases in human colon cancer cells with high metastatic potential. Oncogene. 1997; 15:3083–3090. [PubMed: 9444956]
69. Biscardi JS, Tice DA, Parsons SJ. c-Src, receptor tyrosine kinases, and human cancer. Advances In Cancer Research. 1999; 76:61–119. [PubMed: 10218099]
70. Guo LW, Gao L, Rothschild J, Su B, Gelman IH. Control of Protein Kinase C Activity, Phorbol Ester-induced Cytoskeletal Remodeling, and Cell Survival Signals by the Scaffolding Protein SSeCKS/GRAVIN/AKAP12. J Biol Chem. 2011; 286:38356–38366. [PubMed: 21903576]
71. Gelman IH, Lee K, Tombler E, Gordon R, Lin X. Control of cytoskeletal architecture by the *src*-suppressed C kinase substrate, SSeCKS. Cell Motil Cytoskeleton. 1998; 41:1–17. [PubMed: 9744295]
72. Yeo MG, Partridge MA, Ezratty EJ, Shen Q, Gundersen GG, Marcantonio EE. Src SH2 arginine 175 is required for cell motility: specific focal adhesion kinase targeting and focal adhesion assembly function. Mol Cell Biol. 2006; 26:4399–4409. [PubMed: 16738308]
73. Oneyama C, Hikita T, Enya K, Dobenecker MW, Saito K, Nada S, et al. The lipid raft-anchored adaptor protein Cbp controls the oncogenic potential of c-Src. Mol Cell. 2008; 30:426–436. [PubMed: 18498747]
74. Nethe M, Hordijk PL. A model for phospho-caveolin-1-driven turnover of focal adhesions. Cell Adh Migr. 2011; 5:59–64. [PubMed: 20948305]
75. Del Pozo MA, Balasubramanian N, Alderson NB, Kiosses WB, Grande-Garcia A, Anderson RG, et al. Phospho-caveolin-1 mediates integrin-regulated membrane domain internalization. Nat Cell Biol. 2005; 7:901–908. [PubMed: 16113676]
76. Humphries, MJ. Current Protocols in Cell Biology. Bonifacino, JS.; Dasso, M.; Harford, JB.; Lippincott-Schwartz, J.; Yamada, K., editors. New York: Wiley; 1998. p. 9.1.1-9.1.11.

77. Ross SH, Post A, Raaijmakers JH, Verlaan I, Gloerich M, Bos JL. Ezrin is required for efficient Rap1-induced cell spreading. J Cell Sci. 2011; 124:1808–1818. [PubMed: 21540295]

78. Ory DS, Neugeboren BA, Mulligan RC. A stable human-derived packaging cell line for production of high titer retrovirus/vesicular stomatitis virus G pseudotypes. Proc Natl Acad Sci USA. 1996; 93:11400–11406. [PubMed: 8876147]

79. Bu Y, Gelman IH. v-Src-mediated Down-regulation of SSeCKS Metastasis Suppressor Gene Promoter by the Recruitment of HDAC1 into a USF1-Sp1-Sp3 Complex. J Biol Chem. 2007; 282:26725–26739. [PubMed: 17626016]

80. Akakura S, Nochajski P, Gao L, Sotomayor P, Matsui S, Gelman IH. Rb-dependent cellular senescence, multinucleation and susceptibility to oncogenic transformation through PKC scaffolding by SSeCKS/AKAP12. Cell Cycle. 2010; 9:4656–4665. [PubMed: 21099353]

81. Meng F, Sachs F. Orientation-based FRET sensor for real-time imaging of cellular forces. J Cell Sci. 2012; 125:743–750. [PubMed: 22389408]

82. Li S, Seitz R, Lisanti MP. Phosphorylation of caveolin by src tyrosine kinases. The alpha-isoform of caveolin is selectively phosphorylated by v-Src in vivo. J Biol Chem. 1996; 271:3863–3868. [PubMed: 8632005]

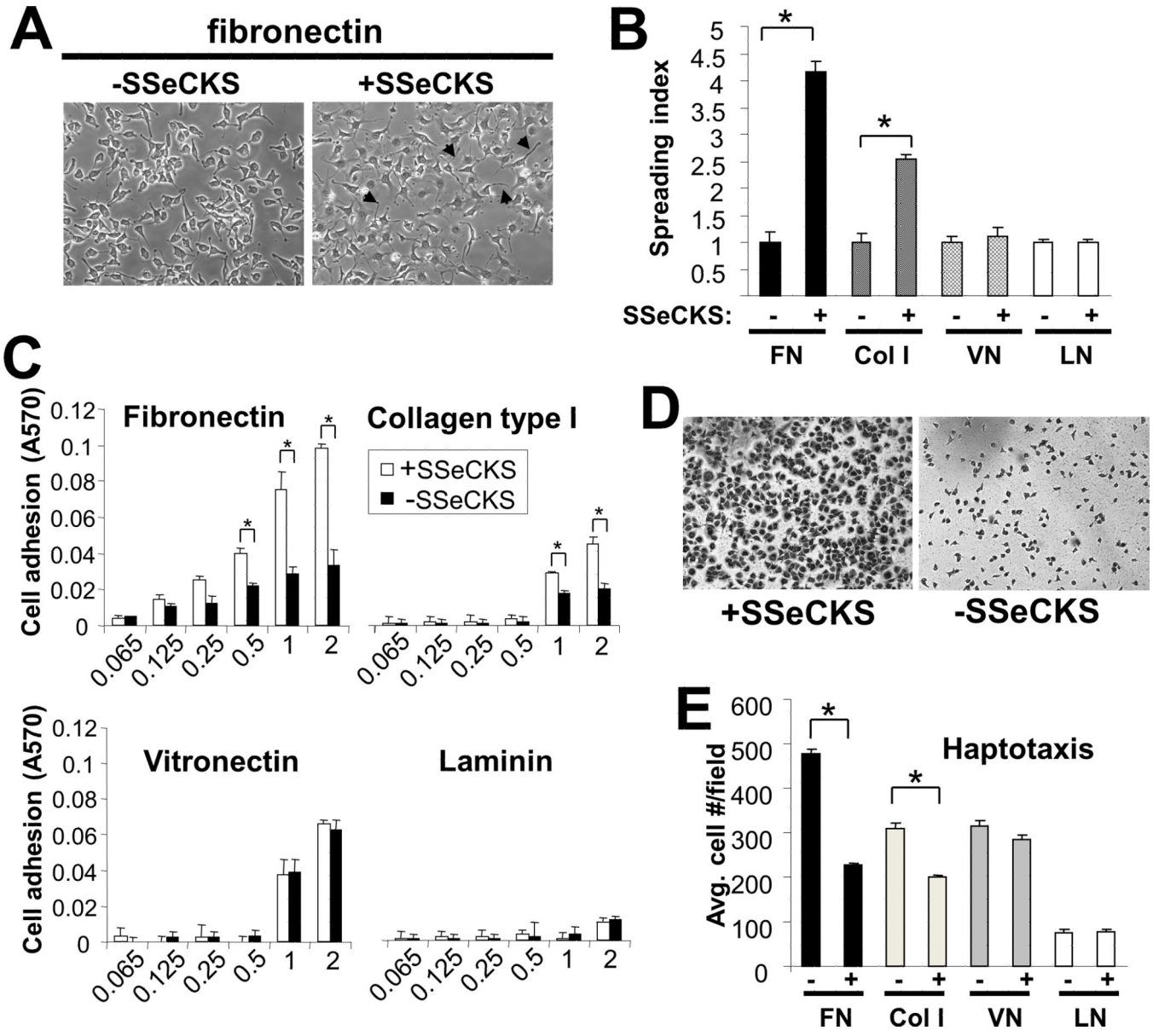


**Fig. 1. SSeCKS increases adhesion toward fibronectin and collagen type I**

**A.** SSeCKS reexpression induces exaggerated pseudofilopodia. MLL/tet-SSeCKS cells were cultured with or without tet overnight, then replated on FN-coated coverslips and allowed to attach for 90 min. Arrows, exaggerated pseudofilopodia. **B.** SSeCKS promotes cell spreading on FN and Col I. MLL/tet-SSeCKS cells grown overnight in the presence or absence of tet were replated onto ECM-coated plates, and the flattened ("spread") cells scored after 60 min. Error bars, SE of 6 independent fields; *, $p < 0.01$. **C.** SSeCKS increases cell attachment toward FN and Col I. MLL/tet-SSeCKS with or without SSeCKS reexpression (white vs. black bars, respectively) were plated for 60 min onto wells coated with increasing ECM concentrations, and the attached cells identified as those remaining after washing with PBS and staining with crystal violet. The extent of retained dye, representing relative cell numbers, was quantified by solubilizing the stained cell with 10%

acetic acid and was measuring by spectrophotometer at 570 nm. Error bars, SE of three independent experiments; *, $p < 0.01$. **D.** SSeCKS-induced cell flattening (left panel) after overnight attachment to FN-coated plates, compared to MLL/tet-SSeCKS cells grown in the presence of tet (right panel). **E.** SSeCKS decreases haptotaxis towards FN and Col I but not to VN or LN. Error bars, SE of 6 independent fields; *, $p < 0.01$.

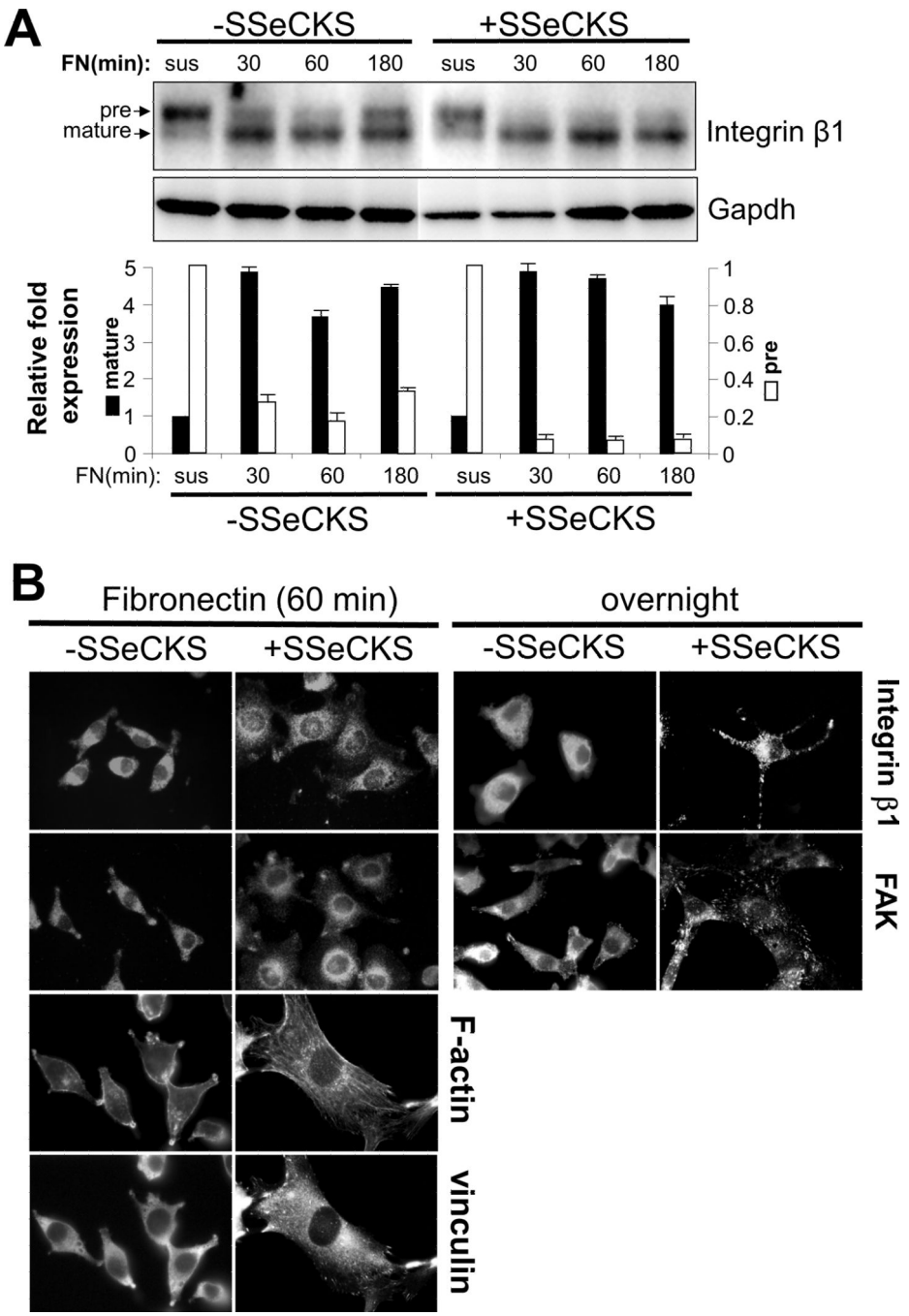


**Fig. 2. SSeCKS induces integrin β1 clustering**

**A.** SSeCKS does not affect integrin β1 expression. MLL/tet-SSeCKS cells incubated with or without tet (− or + SSeCKS, respectively) were plated for various time points on FN or kept in suspension ("sus") and then immunoblotted for integrin β1. The bottom graph shows the relative levels of premature ("pre") or mature integrin β1 from three independent experiments. Error bars, S.E. **B.** MLL/tet-SSeCKS cells were plated onto glass FN-coated coverslips coated for 60 min or overnight in the presence or absence of tet, then fixed and stained for integrin β1, FAK, vinculin or F-actin.

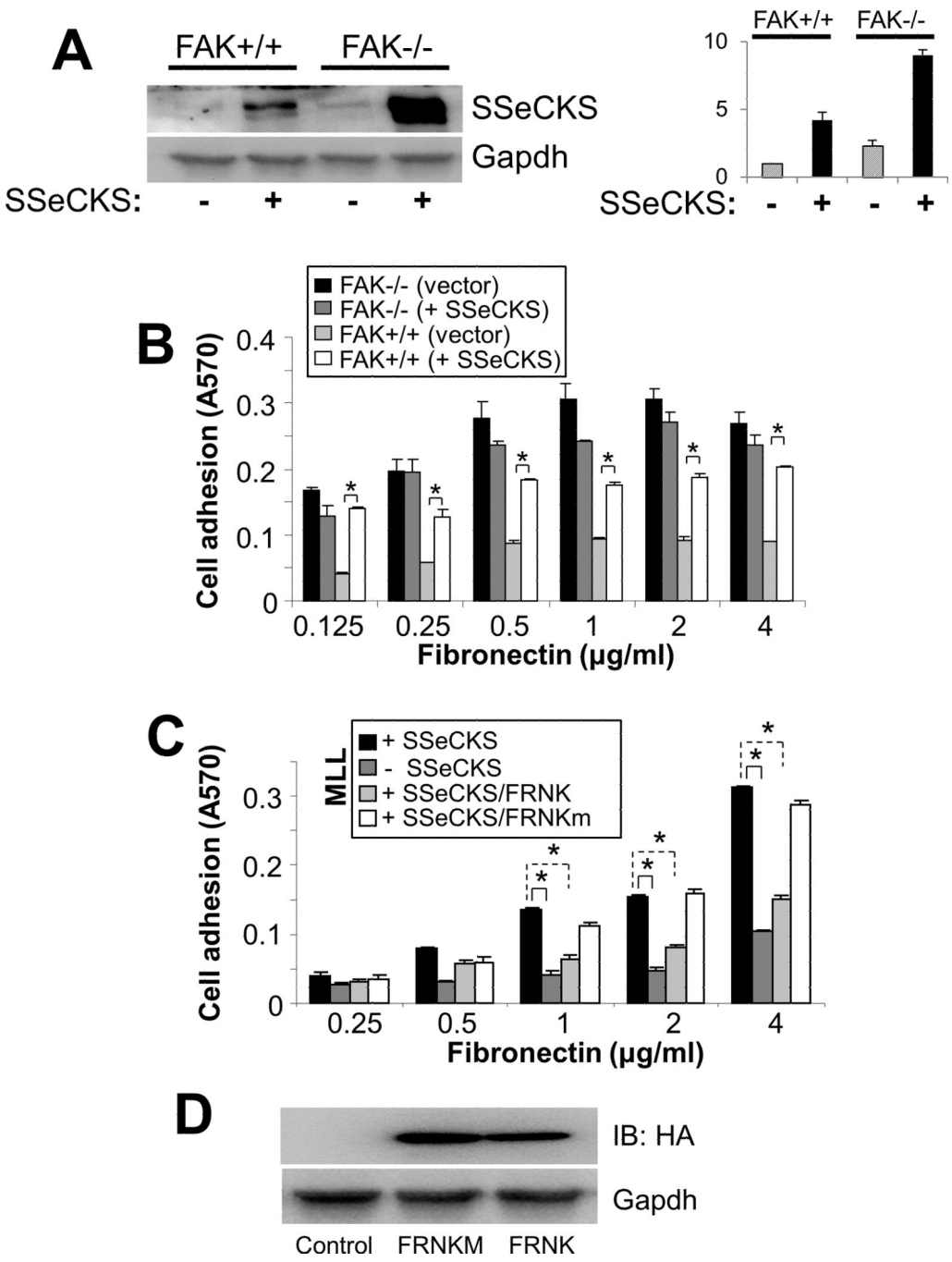


**Fig. 3. SSeCKS regulates cell adhesion through FAK**

**A.** FAK+/+ and FAK−/− MEF transiently transfected with SSeCKS or vector plus pEGFP were analyzed by immunoblotting for SSeCKS (or for Gapdh as a loading control). **B.** SSeCKS increases cell adhesion in FAK+/+ cells. Transfected cells described in Panel A were subjected to adhesion assays as performed in Fig. 1C, where adherent cells were scored as GFP-positive. Error bars, S.E. for duplicates from two independent experiments. *, $p < 0.05$. **C.** FRNK blocks SSeCKS-stimulated cell adhesion. MLL/tet-SSeCKS cells transiently transfected with HA-tagged FRNK or FRNK Ser-1034 (FRNK-KM) plus pEGFP (or pEGFP

alone) were grown in the presence or absence or tet and then plated on various FN concentrations for 1h, followed by assessing cell adhesion levels. Error bars, S.E. for duplicates from two independent experiments. *, $p < 0.05$. **D.** FRNK or FRNKM expression from the experiment in Panel C was confirmed by HA immunoblotting.

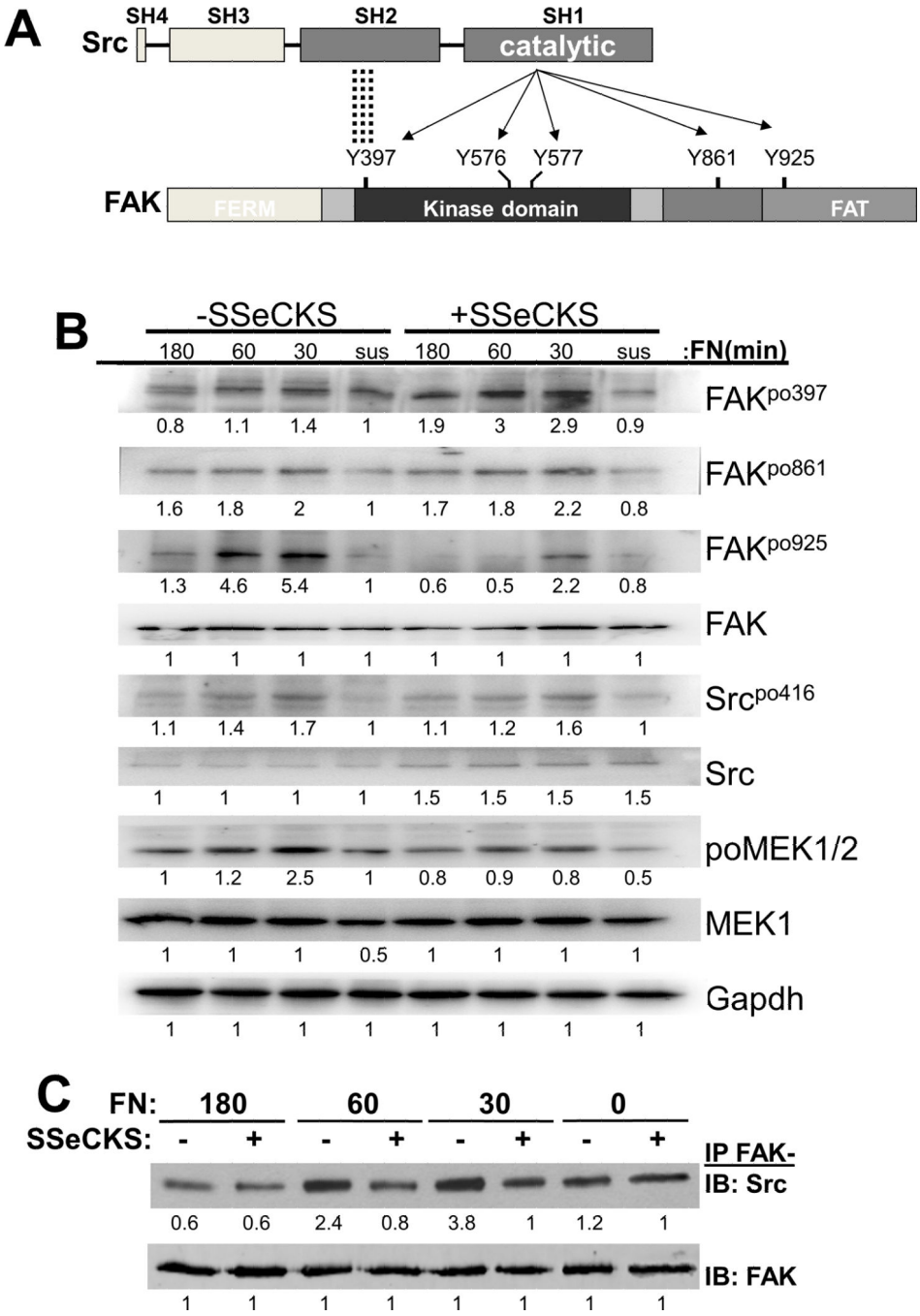


**Fig. 4. SSeCKS differentially controls adhesion-induced FAK and Src phosphorylation**

(A) summary of potential Src phosphorylation sites on FAK (arrows) and the SH2-mediated association of Src with phospho-Y397-FAK (dotted lines). (B) Serum-starved MLL/tet-SSeCKS cells (+/− tet) were adhered to FN coated wells for various times, and then RIPA lysates were analyzed by IB (30 μg protein/lane) for phospho- and/or apo-forms of FAK, Src, Mek or Gapdh. Expression levels were quantified from two independent experiments by digitization (numbers under blots; same in Panel C). (C) RIPA lysates of MLL/tet-SSeCKS cells grown in the presence or absence of tet (− or + SSeCKS, respectively) and then plated

onto FN for various times as in Panel B were IP'ed with FAK Ab-beads (1 mg protein/IP) and then analyzed for Src or FAK by IB.

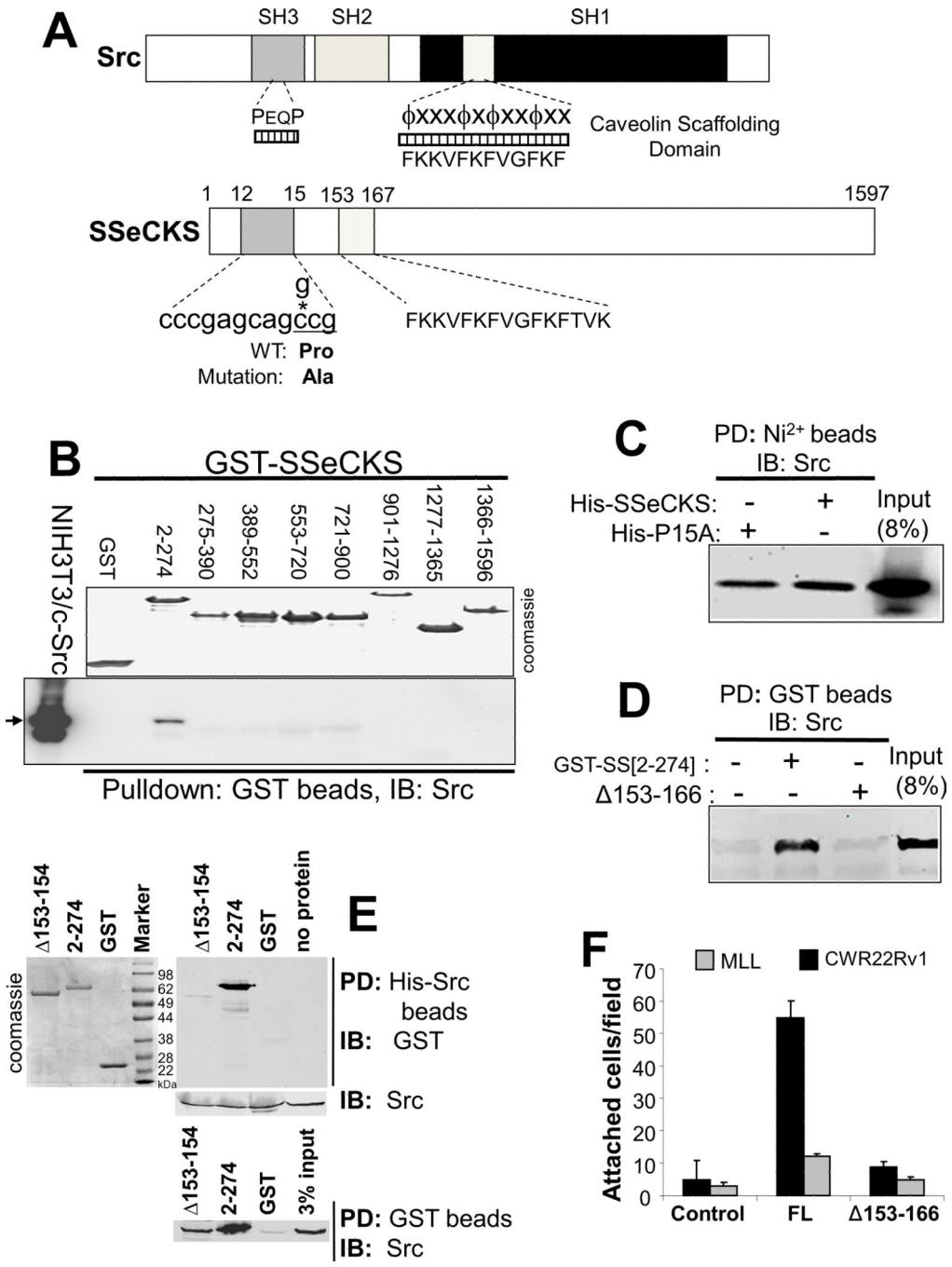


**Fig. 5. Docking of Src to SSeCKS occurs in the N-terminal region of SSeCKS**

**A.** The potential Src binding sequence in SSeCKS. *Top*- Src protein, identifying he Src-homology domains (including a favored SH3 ligand sequence) and the caveolin binding domain (with the binding motif sequence above; residues 82–101: DGIWKASFTTFTVTKYWFYR). *Bottom*- A potential Src-SH3 binding site on SSeCKS ($P^{12}xxP^{15}$; grey box), previously suggested by Tao et al. (56), is shown along with the mutant construct, P15A, and the calveolin-1binding motif homology, $^{153}$FKKVFKFVGFKFTVK$_{167}$. **B.** Beads containing GST or GST-SSeCKS

fusion domains (Coomassie stained proteins in top panel) were incubated with NIH3T3 lysates overexpressing c-Src, washed and then blotted for bound Src protein (bottom panel). A control of NIH3T3/c-Src lysate (10% of the input) blotted for Src is shown at left. **C.** $Ni^{2+}$-beads charged with full-length (FL) or P15A His-SSeCKS proteins were used to pull down (PD) lysates of HEK293T cells transiently overexpressing Src, followed by IB for Src. An aliquot of the lysate representing 8% of the input is shown on the right. **D.** Glutathione-beads charged with GST-SSeCKS[a.a.2–274] or containing an internal deletion of the putative caveolin-1-binding domain (Δ153–166) were used to bind HEK293T/c-Src lysates as shown in Panel C, followed by IB for Src. An aliquot of the lysate representing 8% of the input is shown on the right. **E.** *Upper panel*- $Ni^{2+}$-beads charged with 1 μg/assay of His-tagged Src (GenWay Biotech) were used in pulldown (PD) assays with 5 μg GST, GST-SSeCKS[2–274] or GST-SSeCKS[2–274Δ153–166] (*left panel)* as in Panel D, and then blotted for GST or Src. *Lower panel*- Glutathione-beads charged with GST, GST-SSeCKS[2–274] or GST-SSeCKS[2–274Δ153–166] were used in PD assays with His-Src, followed by Src IB. **F.** GFP-fusions to FL or SSeCKS[Δ153–165] were transiently transfected into MLL or CWR22rv1 cells, and the cells were then assayed for attachment to FN-coated plates as in Fig. 1B. Error bars, S.E. of two independent experiments done in triplicate.

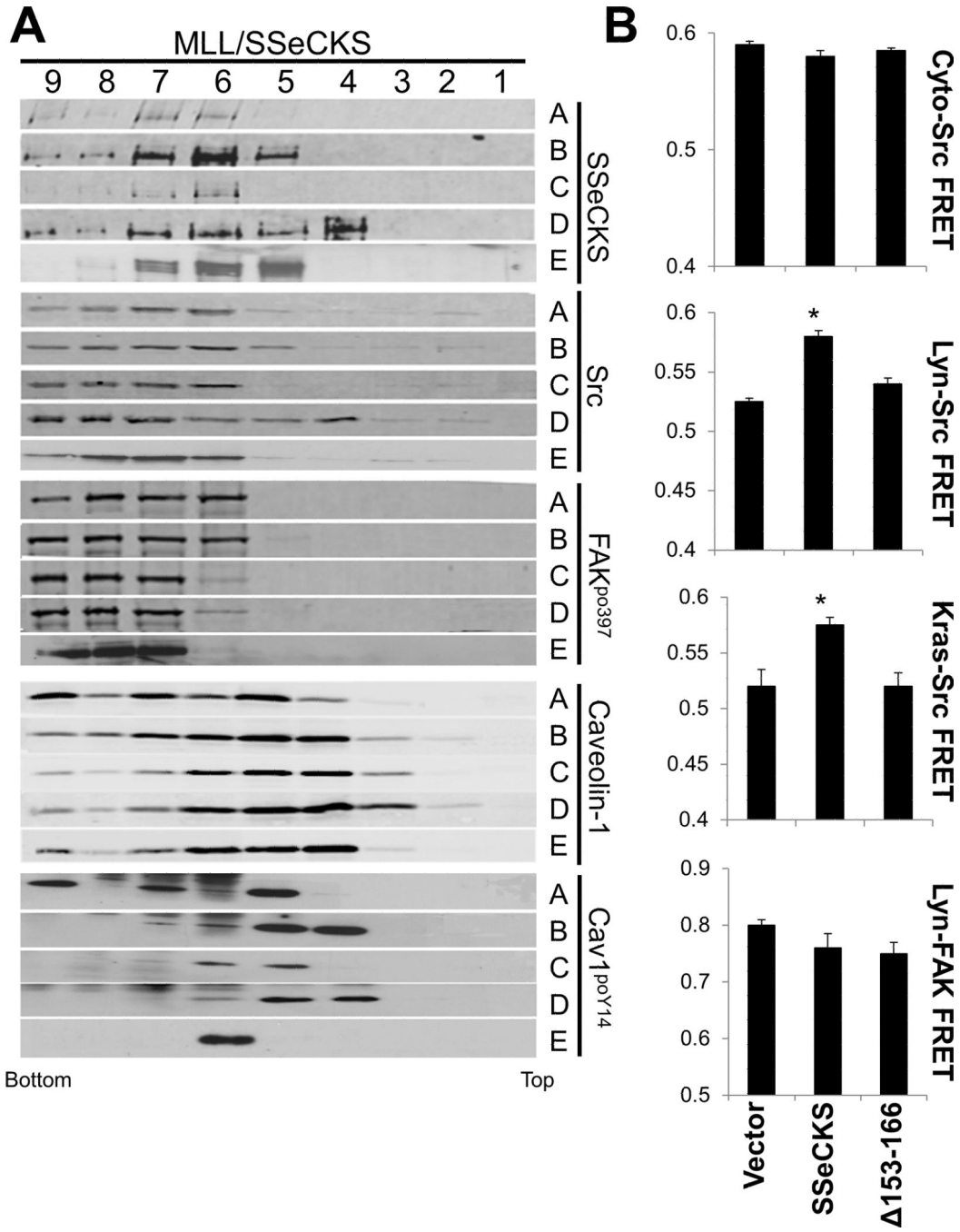


**Fig. 6. SSeCKS drives Src into lipid rafts**

**A.** Stable MLL/tet-SSeCKS cells grown in the presence or absence of tet were either kept in suspension or adhered to FN (10 μg/ml) coated plates for 1h, and after washing with ice-cold PBS, lysates subjected to sucrose gradients were fractionated into heaviest ("bottom", fraction #9) and lightest ("top", fraction #1) as described previously (27) to isolate detergent-resistant caveolin-rich lipid rafts ("light" fractions 4–5). Equal protein aliquots from each fraction were blotted for SSeCKS, Src, FAK$^{poY397}$, Caveolin-1, or Cav-1$^{poY14}$, a known Src phosphorylation site (82). Cell conditions- A: Suspension/tet+, B: Suspension/tet

−, C: Attached/tet+, D: Attached/tet−, E: Attached/tet-/MbCD (10 mM for 1h during FN attachment). **B.** FRET analysis of CWR22Rv1 cells transiently transfected with Src or FAK kinase activity sensors in the cytosol (Cyto-Src), detergent-insoluble, lipid-rafts (Lyn-Src or Lyn-FAK) or general membrane sites (KRas-Src), plus either vector, FL-SSeCKS or SSeCKS[Δ153–166]. Error bars, S.E.; *, P<0.01.

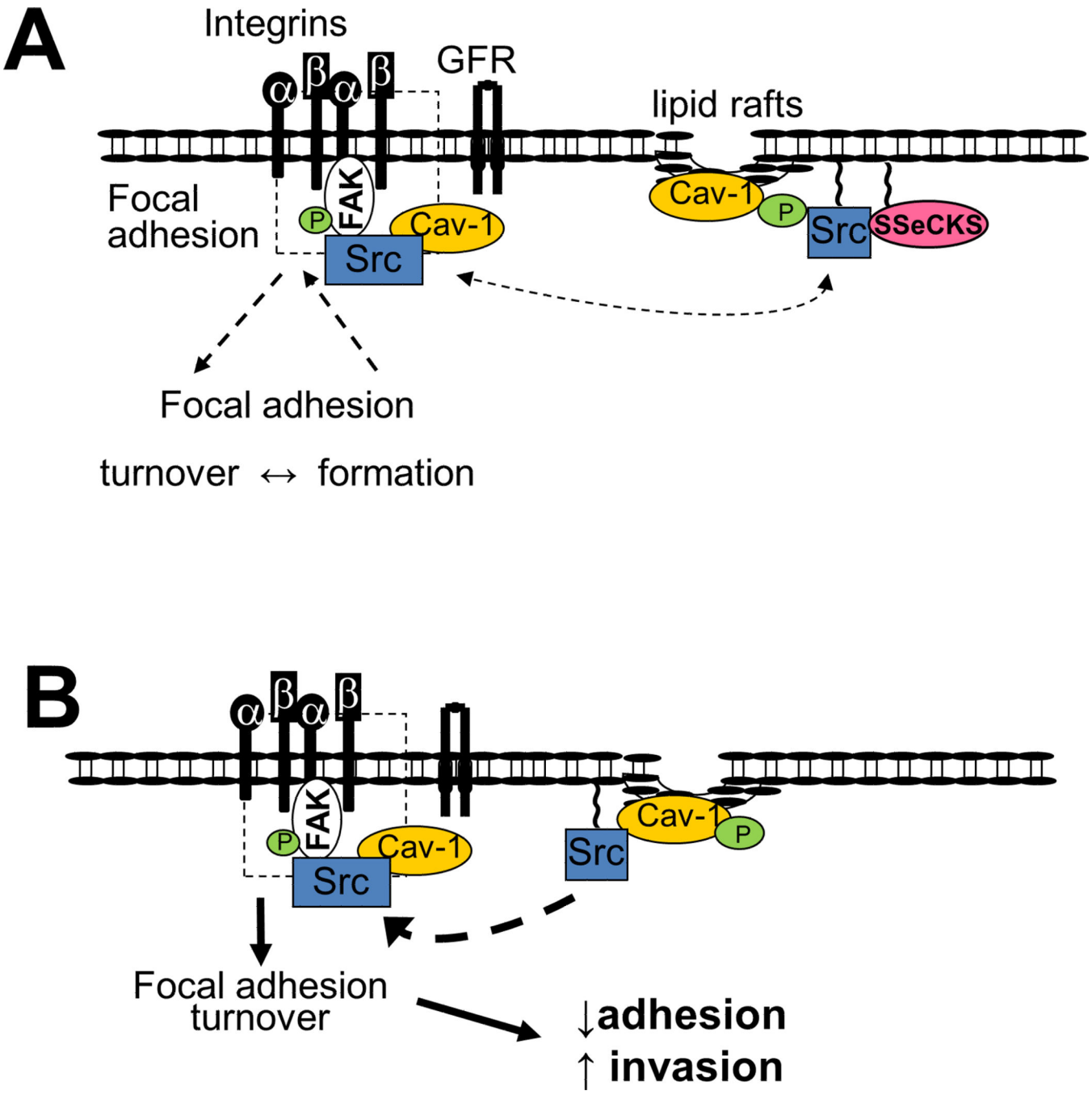


**Fig. 7. Model for SSeCKS-mediated modulation of adhesion-induced FAK/Src signaling**

**A.** Src is scaffolded to lipid rafts by SSeCKS, where it phosphorylates Cav-1 on Y14. As postulated by Nethe and Hordijk (74), normal adhesion signaling induces FAK autophosphorylation, triggering the Rac1-dependent translocation of Src/Cav-1$^{poY14}$ to FAK-containing focal adhesion complexes and the subsequent association with and phosphorylation of FAK by Src on secondary sites such as Y925. The subsequent dephosphorylation of Cav-1 triggers Cav-1 degradation, focal adhesion turnover and cell motility. SSeCKS likely sustains a dynamic balance between Src/Cav-1 pools in lipid rafts

vs. focal adhesions, thereby assuring transience to the focal adhesion turnover. **B.** In cancer cells exhibiting SSeCKS downregulation, Src/Cav-1 translocation to focal adhesions is over-activated, thereby facilitating in higher levels of FAK autophosphorylation and transphosphorylation by Src, and resulting in sustained kinetic focal adhesion turnover, decreased adhesion and increased oncogenic motility and invasiveness.